Journal of Hepatocellular Carcinoma

Dovepress
Taylor & Francis Group

Open Access Full Text Article

ORIGINAL RESEARCH

Prognostic Value of Gd-BOPTA Enhanced MRI in Solitary Resected Hepatocellular Carcinoma Without Microvascular Invasion

Juan Zhang[1,2,*], Hongmei Luo[2,*], Yinqiao Li[2,*], Yayuan Feng[2], Xingpeng Pan[2], Beilei Ouyang[2], Guihong Nian[2], Ningyang Jia[2], Yonggang Li[1,3]

[1]Department of Radiology, The First Affiliated Hospital of Soochow University, Suzhou City, Jiangsu Province, 215006, People's Republic of China; [2]Department of Radiology, Eastern Hepatobiliary Surgery Hospital, Third Affiliated Hospital of Naval Medical University, Shanghai, 200438, People's Republic of China; [3]Institute of Medical Imaging, Soochow University, Suzhou City, Jiangsu Province, 215000, People's Republic of China

*These authors contributed equally to this work

Correspondence: Ningyang Jia; Yonggang Li, Email ningyangjia@163.com; liyonggang@suda.edu.cn

Objective: This study aims to evaluate the prognostic predictive efficacy of Gadobenate dimeglumine (Gd-BOPTA)-enhanced magnetic resonance imaging (MRI) in patients with solitary hepatocellular carcinoma (HCC) without microvascular invasion (MVI) and to investigate the potential clinical and imaging parameters for stratifying the risk of recurrence following hepatectomy.

Methods: This retrospective study included 134 patients with histopathologically confirmed solitary HCC without microvascular invasion (MVI) from two hospital districts, which divided into the training cohort and validation cohort. MRI features were independently assessed by two radiologists. Univariate and multivariate Cox regression analyses were conducted to identify independent risk factors associated with recurrence-free survival (RFS). A nomogram was developed based on these factors, and its performance was validated in the validation cohort. RFS was analyzed using Kaplan–Meier curves and the Log rank test.

Results: The median RFS for the 134 patients was 45.7 months, with 41.8% of patients experiencing tumor recurrence after hepatectomy. Univariate Cox regression analysis identified hepatitis Be antigen (HBeAg) positivity, tumor size, tumor growth subtype, non-peripheral washout, nodule-in-nodule architecture, mosaic architecture, and intratumoral arteries as significant risk factors for RFS. Multivariate Cox regression analysis revealed that HBeAg positive, tumor growth subtype, non-peripheral washout, mosaic architecture, and internal arteries were independent prognostic factors for RFS in patients with solitary HCC without MVI. The nomogram based on these variables demonstrated good predictive accuracy, with concordance indices (C-index) of 0.740 and 0.701 in the training and validation cohorts, respectively. Additionally, patients in the high-risk group exhibited significantly lower RFS compared to those in the low-risk group.

Conclusion: A model incorporating Gd-BOPTA-enhanced MRI and clinical features can effectively predict RFS in solitary HCC patients without MVI and assist in risk stratification for recurrence after hepatectomy.

Keywords: hepatocellular carcinoma, magnetic resonance imaging, recurrence

Introduction

Hepatocellular carcinoma (HCC) is the sixth most common malignant tumor globally and ranks third in cancer-related mortality.[1] Surgical resection remains the primary treatment for HCC; however, the 5-year postoperative recurrence rate is alarmingly high, ranging from 50% to 70%.[2] Although liver transplantation and ablation are also considered potentially curative treatments, many patients still experience recurrence due to local invasion or metastatic spread.[3] The current studies focus on predicting microvascular invasion (MVI) status and evaluating the prognosis of patients with MVI-positive HCC, with expanded surgical and ablative margin often recommended for MVI-positive patients.[4] However, many MVI-negative patients still develop postoperative recurrence with unfavorable prognosis, yet the prognostic factors for this population remain poorly investigated.

Received: 9 April 2025
Accepted: 8 July 2025
Published: 18 July 2025

Several studies have identified magnetic resonance imaging (MRI) features—such as tumor size, multiplicity, mosaic architecture, corona enhancement, and peritumoral hypointensity on the hepatobiliary phase—as significant prognostic indicators for HCC.[5,6] Gadobenate dimeglumine (Gd-BOPTA) is a contrast agent that enters hepatocytes via organic anion-transporting polypeptides (OATP1/3) and is subsequently excreted into the biliary tree during the hepatobiliary phase.[7] Gd-BOPTA offers advantages over other agents, including distinct hepatobiliary and dynamic phases[8] and hepatic uptake that is independent of age.[9] Previous studies have demonstrated the utility of Gd-BOPTA in assessing liver function,[10] cirrhosis progression,[9] HCC pathological grading,[11] and the prediction of MVI.[6] However, to our knowledge, the predictive value of Gd-BOPTA-enhanced MRI for the prognosis in HCC patients without MVI has not been reported.

Thus, this study aims to evaluate the prognostic efficacy of preoperative clinical parameters and Gd-BOPTA-enhanced MRI features in HCC patients without MVI, with the potential to develop a risk stratification model for recurrence prediction.

Materials and Methods

Patients

The study was conducted by the Declaration of Helsinki. The study protocol was approved by the Ethics Committee of the Third Affiliated Hospital of Naval Medical University (approval code: EHBHKY2022-H-P002). As this study was a retrospective analysis that did not involve active patient participation or any intervention in patient therapy, the requirement for informed consent was waived. We retrospectively collected data from 301 patients with hepatocellular carcinoma (HCC) who underwent Gd-BOPTA-enhanced MRI within 2 weeks prior to curative resection between January 2016 and August 2019. The inclusion criteria were as follows: (1) a solitary tumor, (2) MRI examination within two weeks before surgery, and (3) liver resection with pathological confirmation of HCC without microvascular invasion (MVI), (4) no history of any related treatment before surgery. The exclusion criteria were as follows: (1) multiple tumors, (2) pathological confirmation of MVI-positive HCC, (3) history of prior treatments, (4) inadequate MR image quality, and (5) incomplete clinical or follow-up data after curative resection.

MRI Examination

All MRI examinations were performed using a GE Optima MR360 1.5T system (GE Healthcare, USA) with an eight-channel abdominal coil. Patients fasted for 4 hours prior to the scan. The non-contrast MRI protocol included axial in-phase and opposed-phase T1-weighted imaging, axial fat-suppressed T2-weighted imaging, and diffusion-weighted imaging (DWI) with b-values of 0 and 600 s/mm², using a slice thickness of 6 mm. Contrast-enhanced imaging consisted of arterial phase (AP) scans at 20–30 seconds, portal venous phase (PVP) at 50–60 seconds, and delayed phase (DP) at 90–120 seconds after contrast injection. Hepatobiliary phase (HBP) images were acquired 60 minutes post-contrast with a slice thickness of 2.5 mm. The field of view (FOV) was set to 420×420 mm. Gd-BOPTA (MultiHance, Bracco) was administered using a power injector at a dose of 0.1 mL/kg, with an injection rate of 2.0 mL/s, followed by a 20 mL flush of 0.9% sterile saline.

Imaging Analysis

All MR images were independently reviewed by two radiologists (ZJ and PXP, with 9 and 19 years of experience in liver MRI, respectively), who were blinded to clinical and follow-up information. Interobserver agreement for MRI features was assessed during the first independent analysis. In cases of disagreement, the two radiologists convened to reach consensus.

According to the Liver Imaging Reporting and Data System (LI-RADS) criteria (Version 2018), the following Gd-BOPTA MRI features were evaluated: (a) Non-rim arterial phase hyperenhancement: Non-rim-like enhancement in the arterial phase; (b) Nonperipheral washout: Tumor enhancement that attenuates relative to adjacent liver tissue in the portal or delayed phase; (c) Enhancing capsule: Enhancement of the tissue rim during the portal venous and delayed phases; (d) Nodule-in-nodule architecture: Smaller inner nodules within larger nodules, with distinct imaging

characteristics; (e) Mosaic architecture: Presence of internal nodules with varying components or combinations within a mass; (f) Fat in mass: Excess fat within the mass compared to adjacent liver tissue; (g) Blood products in mass: Evidence of intra-tumor hemorrhage, excluding other confounding factors; (h) Rim arterial phase hyperenhancement: Peripheral enhancement most pronounced in the arterial phase; (i) Delayed central enhancement: Progressive enhancement in the central region during the delayed phase; (j) Corona enhancement: Peritumoral enhancement in the late arterial or early portal venous phases; (k) Hepatobiliary phase hypointensity: Signal intensity lower in tumors than in the liver during the hepatobiliary phase; (l) Mild-moderate T2 hyperintensity: Tumors with higher intensity on T2-weighted imaging than the surrounding liver; (m) Targetoid restriction: Diffusion restriction in the tumor periphery, with less restricted diffusion at the center; (n) Restricted diffusion: Intensity on DWI that is definitively higher than liver and not solely attributable to T2 shine-through; (o) Tumor growth subtype: Single nodular type, single nodular type with extranodular growth, and multiple confluent nodules;[12] (p) Non-smooth tumor margin: Defined by tumor margins with budding portions; (q) Internal arteries: Enhanced vascularity within the tumor during the arterial phase; (r) Peritumoral hypointensity on HBP: Irregular or wedge-shaped areas of ypointensity beyond the tumor edge during the hepatobiliary phase.

Clinical Data and Histopathology Analysis

Clinical data were extracted from the electronic medical record system, including variables such as gender, age, hepatitis B surface antigen(HBsAg), hepatitis Be antigen(HBeAg), alpha-fetoprotein (AFP), alanine aminotransferase, aspartate aminotransferase, gamma-glutamyl transpeptidase, alkaline phosphatase, total bilirubin, direct bilirubin, and albumin levels.

Follow-up and Study Endpoint

The primary endpoint of this study was tumor recurrence. Patients were followed up starting 1 month after radical resection, with follow-up every 3 months for the first 2 years, and annually thereafter. Follow-up evaluations included serum AFP testing and imaging assessments, such as contrast-enhanced ultrasound, CT, or MRI. Data recorded included the date of surgery, recurrence, metastasis, or last follow-up to calculate recurrence-free survival (RFS). The diagnosis of recurrence was based on positive imaging findings and persistently elevated AFP levels postoperatively. The follow-up period ended in September 2024.

Statistical Analysis

Statistical analyses were performed using SPSS software (version 26.0; IBM) and R software (version 3.6.1). Continuous variables were compared using the Student's *t*-test or Mann–Whitney *U*-test, which depended on the distribution of the data. Categorical variables were analyzed using the χ^2-test. The Cox proportional hazard model was used to identify potential predictors of recurrence. Survival analysis was performed using the Kaplan-Meier method, with differences assessed by the Log rank test. P-values less than 0.05 were considered statistically significant. The consistency index (C-index) was used to assess the predictive accuracy of recurrence.

Results

Patients Characteristics

Ultimately, 134 patients were included in the final study population, consisting of 107 patients from the main hospital and 37 from the branch hospital, all with pathologically confirmed HCC without MVI (Figure 1). The characteristics of the study cohort are summarized in Table 1. A total of 134 patients (mean age: 55.0 ± 11.2 years; 111 males, 23 females) with surgically confirmed solitary hepatocellular carcinoma (HCC) without microvascular invasion (MVI) were included. Among these, 85.8% (115/134) were hepatitis B surface antigen (HBsAg)-positive, 25.4% (34/134) were hepatitis B e-antigen (HBeAg)-positive, and 55.2% (74/134) had pathologically confirmed cirrhosis. Table 1 also summarizes the clinical and MRI characteristics of the patients in both the training and validation cohorts, with no significant differences found between the clinicopathologic and MRI features of the two cohorts (all $p > 0.05$).

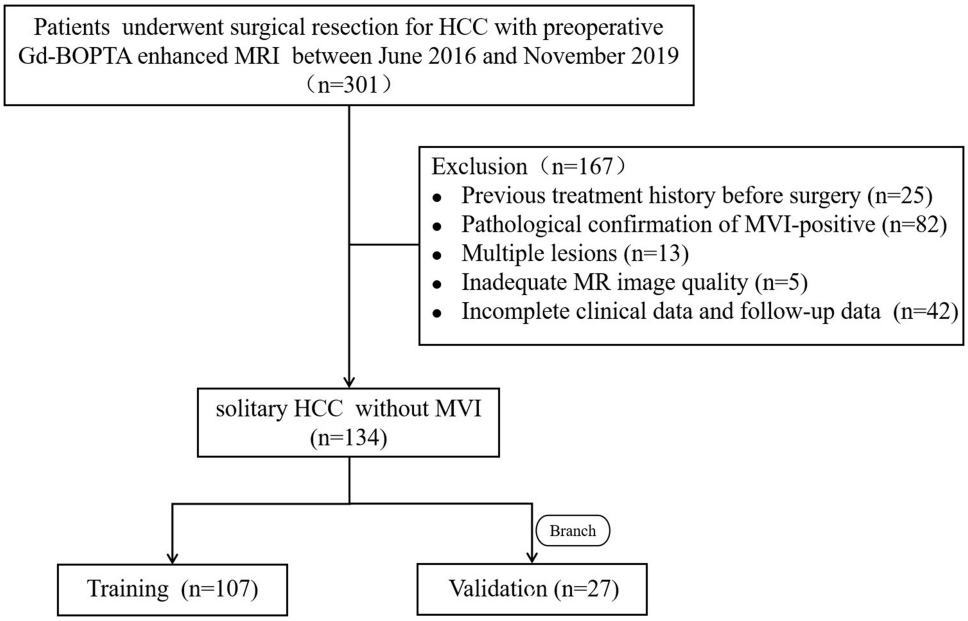

Figure 1 Flowchart of the study population.

Recurrence-Free Survival (RFS) in Solitary HCC Patients Without MVI

The median recurrence-free survival of the 134 patients was 45.7 months (1.0–75 months). 41.80% (56/134) of patients experienced tumor recurrence during the period. Among them, the median RFS was 20.0 months in the training cohort and 20.1 months in the validation cohort, respectively. Additionally, the 1-year, 3-year, and 5-year RFS rates were 80.4%, 65.4%, and 57.0% in the training cohort and 88.9%, 66.7%, and 63.0%in the validation cohort, respectively.

Identification Predictors for RFS

Univariate Cox regression analysis found that HBeAg, tumor size, tumor growth subtype, non-peripheral washout, nodule-in-nodule architecture, mosaic architecture, delayed central enhancement, and internal arteries were significant

Table 1 Clinicopathologic Characteristics and MRI Features of the Training and Validation Cohort

Characteristic	Total (n=134)	Training (n=107)	Validation (n=27)	p Value
Age (years)	55.0 ± 11.2	55.0 ± 11.1	55.3 ± 12.1	0.909
Gender				0.717
Male	111 (82.8)	88 (82.2)	23 (85.2)	
Female	23 (17.2)	19 (17.8)	4 (14.8)	
HBsAg				0.916
Absent	19 (14.2)	15 (14.0)	4 (14.8)	
Present	115 (85.8)	92 (86.0)	23 (85.2)	
HBeAg				0.941
Absent	100 (74.6)	80 (74.8)	20 (74.1)	
Present	34 (25.4)	27 (25.2)	7 (25.9)	
Cirrhosis				0.033
Absent	60 (44.8)	43 (40.2)	17 (63.0)	
Present	74 (55.2)	64 (59.8)	10 (37.0)	
Serum AFP level				0.362
≤400 ng/mL	112 (83.6)	91 (85.0)	21 (77.8)	
>400 ng/mL	22 (16.4)	16 (15.0)	6 (22.2)	

(*Continued*)

Table 1 (Continued).

Characteristic	Total (n=134)	Training (n=107)	Validation (n=27)	p Value
Serum PT level	12.0 ± 1.0	12.1 ± 1.1	11.5 ± 0.8	0.016
Serum ALT level	27 (19, 39)	27 (19, 38.3)	20 (16, 54)	0.478
Serum AST level	25 (19, 33)	25.5 (19, 32.3)	23 (16, 30)	0.579
Serum GGT level	38 (24, 77.3)	39 (23, 75.8)	32 (24, 79)	0.711
Serum ALB level	42.7 ± 6.6	43.0 ± 6.0	41.1 ± 8.5	0.170
Serum pro-ALB level	215.7 ± 72.4	216.7 ± 73.8	211.8 ± 68.2	0.756
Serum TBiL level	13.9 (11.3, 18.0)	14.4 (12, 18.1)	12.6 (9.6, 15.3)	0.021
Serum dBiL level	5.3 (4.2, 7.1)	5.4 (4.2, 7.2)	5 (4.1, 6.2)	0.472
Edmondson-Steiner grade				0.742
I–II	22 (16.4)	17 (15.9)	5 (18.5)	
III–IV	112 (83.6)	90 (84.1)	22 (81.5)	
Tumor size	3.6 ± 1.8	3.6 ± 1.9	3.6 ± 1.7	0.829
Tumor growth subtype				0.677
Single nodular	106 (79.1)	84 (78.5)	22 (81.5)	
Single nodular with extranodular growth	12 (9.0)	9 (8.4)	3 (11.1)	
Confluent multinodular	16 (11.9)	14 (13.1)	2 (7.4)	
Non-rim arterial phase hyperenhancement				0.093
Absent	25 (18.7)	23 (21.5)	2 (7.4)	
Present	109 (81.3)	84 (78.5)	25 (92.6)	
Non-peripheral washout				0.081
Absent	41 (30.6)	29 (27.1)	12 (44.4)	
Present	93 (69.4)	78 (72.9)	15 (55.6)	
Enhancing capsule				0.181
Absent	60 (44.8)	51 (47.7)	9 (33.3)	
Present	74 (55.2)	56 (52.3)	18 (66.7)	
Non-enhancing capsule				0.691
Absent	127 (94.8)	101 (94.4)	26 (96.3)	
Present	7 (5.2)	6 (5.6)	1 (3.7)	
Nodule-in-nodule architecture				0.134
Absent	116 (86.6)	95 (88.8)	21 (77.8)	
Present	18 (13.4)	12 (11.2)	6 (22.2)	
Mosaic architecture				0.500
Absent	101 (75.4)	82 (76.6)	19 (70.4)	
Present	33 (24.6)	25 (23.4)	8 (29.6)	
Fat in mass, more than adjacent liver				0.169
Absent	107 (79.9)	88 (82.2)	19 (70.4)	
Present	27 (20.1)	19 (17.8)	8 (29.6)	
Blood products in mass				0.589
Absent	104 (77.6)	82 (76.6)	22 (81.5)	
Present	30 (22.4)	25 (23.4)	5 (18.5)	
Rim arterial phase hyperenhancement				0.356
Absent	117 (87.3)	92 (86.0)	25 (92.6)	
Present	17 (12.7)	15 (14.0)	2 (7.4)	
Peripheral washout				0.410
Absent	128 (95.5)	103 (96.3)	25 (92.6)	
Present	6 (4.5)	4 (3.7)	2 (7.4)	
Delayed central enhancement				0.828
Absent	128 (95.5)	102 (95.3)	26 (96.3)	
Present	6 (4.5)	5 (4.7)	1 (3.7)	

(*Continued*)

https://doi.org/10.2147/JHC.S530701

Table 1 (Continued).

Characteristic	Total (n=134)	Training (n=107)	Validation (n=27)	p Value
Targetoid restriction				0.410
Absent	128 (95.5)	103 (96.3)	25 (92.6)	
Present	6 (4.5)	4 (3.7)	2 (7.4)	
Hepatobiliary phase hypointensity				0.558
Absent	20 (14.9)	15 (14.0)	5 (18.5)	
Present	114 (85.1)	92 (86.0)	22 (81.5)	
Mild-moderate T2 hyperintensity				0.419
Absent	10 (7.5)	7 (6.5)	3 (11.1)	
Present	124 (92.5)	100 (93.5)	24 (88.9)	
Corona enhancement				0.652
Absent	121 (90.3)	96 (89.7)	25 (92.6)	
Present	13 (9.7)	11 (10.3)	2 (7.4)	
Restricted diffusion				0.315
Absent	13 (9.7)	9 (8.4)	4 (14.8)	
Present	121 (90.3)	98 (91.6)	23 (85.2)	
Fat sparing in solid mass				0.614
Absent	133 (99.3)	106 (99.1)	27 (100)	
Present	1 (0.7)	1 (0.9)	0 (0)	
Iron sparing in solid mass				0.308
Absent	130 (97.0)	103 (96.3)	27 (100)	
Present	4 (3.0)	4 (3.7)	0 (0)	
Non-smooth tumor margin				0.384
Absent	106 (79.1)	83 (77.6)	23 (85.2)	
Present	28 (20.9)	24 (22.4)	4 (14.8)	
Internal arteries				0.315
Absent	121 (90.3)	98 (91.6)	23 (85.2)	
Present	13 (9.7)	9 (8.4)	4 (14.8)	
Peritumoral hypointensity on HBP				0.692
Absent	116 (86.6)	92 (86.0)	24 (88.9)	
Present	18 (13.4)	15 (14.0)	3 (11.1)	

Abbreviations: AFP, alpha-fetoprotein; PT, prothrombin time; ALT, alanine transaminase; AST, aspartate transaminase; GGT, γ-glutamyl transpeptidase; ALB, albumin; proALB, pro-albumin; Tbil, total bilirubin; dTbil, direct bilirubin; HBP, hepatobiliary phase.

risk factors with the RFS in solitary HCC patients without MVI. Among them, HBeAg (HR, 3.547; 95% CI: 1.870, 6.727; p<0.001), tumor growth subtype (HR, 1.576; 95% CI: 1.087, 2.287; p=0.016), non-peripheral washout (HR, 0.505; 95% CI: 0.266, 0.958; p=0.037), mosaic architecture (HR, 3.155; 95% CI: 1.636, 6.083; p=0.001) and internal arteries (HR, 2.201; 95% CI: 0.938, 5.167; p=0.070) were associated with RFS at the multivariate Cox regression analysis (Table 2). Representative images of recurrence are shown in Figures 2 and 3. The Kaplan-Meier curves of the prognostic risk factors for RFS are shown in Figure 4.

Construction of the RFS Nomogram

The significant prognostic risk factors identified by the multivariate Cox regression analysis in the training cohort were further utilized to construct the RFS nomogram (Figure 5). The concordance index (C-index) of the RFS nomogram was 0.740 in the training cohort and 0.701 in the validation cohort, indicating good predictive accuracy. Additionally, we calculated individual patient risk scores and categorized patients into high- and low-risk groups, with a cut-off value of −6.96. On analysis, it was found that patients in the low-risk group had significantly higher RFS rates than those in the high-risk group. This result was validated in the validation cohort, with p-values of < 0.0001 in the training cohort and 0.0052 in the validation cohort (Figure 6).

Table 2 Univariate and Multivariate Cox Regression Analysis for RFS in the Training Group

Characteristic	Univariate Analysis		Multivariate Analysis	
	HR (95% CI)	p Value	HR (95% CI)	p Value
Age	1.015 (0.989, 1.043)	0.264		
Gender	0.778 (0.348, 1.740)	0.541		
HBsAg	2.101 (0.753, 5.865)	0.156		
HBeAg	2.490 (1.364, 4.548)	0.003*	3.547 (1.870, 6.727)	<0.001
AFP	1.42 (0.962, 3.921)	0.064		
ALT	1.003 (0.989, 1.017)	0.717		
AST	1.000 (0.985,1.014)	0.975		
GGT	1.000 (0.997, 1.004)	0.829		
ALB	1.001 (0.949, 1.057)	0.964		
Pro-ALB	0.996 (0.991, 1.000)	0.051		
TBiL	1.008 (0.962, 1.056)	0.743		
dBiL	0.994 (0.966, 1.023)	0.687		
Edmondson-Steiner grade	1.732 (0.684, 4.383)	0.247		
Tumor size	2.221 (1.184, 4.168)	0.013*		
Tumor growth subtype	1.626 (1.144, 2.312)	0.007*	1.576 (1.087, 2.287)	0.016
Non-rim arterial phase hyperenhancement	0.526 (0.276, 1.002)	0.051		
Non-peripheral washout	0.518 (0.284, 0.943)	0.031*	0.505 (0.266, 0.958)	0.037
Enhancing capsule	1.352 (0.751,2.432)	0.315		
Non-enhancing capsule	1.332 (0.413, 4.298)	0.631		
Nodule-in-nodule architecture	3.567 (1.706, 7.455)	0.001*		
Mosaic architecture	3.009 (1.657, 5.465)	<0.001*	3.155 (1.636, 6.083)	0.001
Fat in mass, more than adjacent liver	0.737 (0.330, 1.649)	0.458		
Blood products in mass	1.477 (0.777, 2.808)	0.234		
Rim arterial phase hyperenhancement	1.902 (0.916, 3.949)	0.084		
Peripheral washout	1.878 (0.582, 6.058)	0.292		
Delayed central enhancement	3.245 (1.154, 9.126)	0.026*		
Targetoid restriction	0.571 (0.079, 4.146)	0.580		
Hepatobiliary phase hypointensity	0.540 (0.260, 1.120)	0.098		
Mild-moderate T2 hyperintensity	0.467 (0.184, 1.183)	0.108		
Corona enhancement	0.522 (0.162, 1.684)	0.277		
Restricted diffusion	0.711 (0.301, 1.679)	0.436		
Fat sparing in solid mass	0.049 (0, 5734.881)	0.612		
Iron sparing in solid mass	0.437 (0.060, 3.172)	0.413		
Non-smooth tumor margin	1.159 (0.589, 2.284)	0.669		
Internal arteries	3.803 (1.755, 8.242)	0.001*	2.201 (0.938, 5.167)	0.070
Peritumoral hypointensity on HBP	1.482 (0.691, 3.179)	0.312		

Note:* indicates statistical significance ($p < 0.05$).

Abbreviations: AFP, alpha-fetoprotein; ALT, alanine transaminase; AST, aspartate transaminase; GGT, γ-glutamyl transpeptidase; ALB, albumin; proALB, pro-albumin; Tbil, total bilirubin; dTbil, direct bilirubin; HBP, hepatobiliary phase.HBP, hepatobiliary phase; CI, confidence interval; HR, hazard ratios.

Discussion

In this study, we aimed to evaluate the predictive efficacy of preoperative Gd-BOPTA imaging features and clinical indicators to predict the prognosis of hepatocellular carcinoma (HCC) patients without microvascular invasion (MVI). Our results identified hepatitis B e-antigen positivity (HBeAg), tumor growth subtype, non-peripheral washout, mosaic architecture, and internal arteries as significant prognostic risk factors for recurrence-free survival (RFS). We subsequently developed a model incorporating these variables and conducted stratified risk analyses, suggesting that the model can be effectively utilized for prognostic prediction in HCC patients without MVI. This research provides valuable insights for clinical decision-making and individualized treatment planning in this patient population.

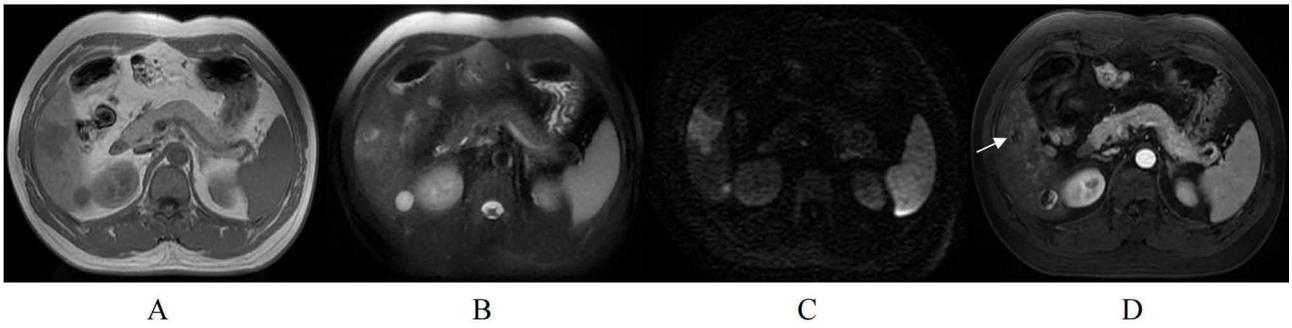

Figure 2 The images show a 41-year-old male diagnosed with HCC without MVI, who experienced recurrence 7 months after hepatectomy. (**A**) The tumor growth subtype was multiple confluent nodules on T1-weighted imaging (T1WI); (**B**) Heterogeneous mass with mosaic architecture on T2-weighted imaging (T2WI); (**C**) The lesion appears hyperintense on diffusion-weighted imaging (DWI); (**D**) Heterogeneous and marked enhancement on the arterial phase, with the artery (white arrow) visible within the tumor.

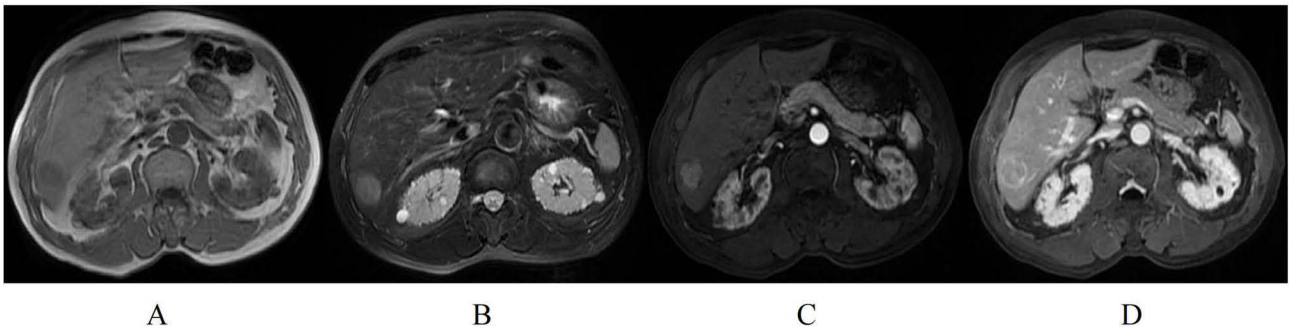

Figure 3 MR images of a 71-year-old male who did not experience postoperative recurrence. (**A**) Single nodular with homogeneous, slightly low signal on T1WI; (**B**) The lesion of homogeneous slightly high signal on T2WI; (**C**) Non-rim arterial phase hyperenhancement (APHE) on the arterial phase; (**D**) Non-peripheral washout on the portal venous phase.

The study indicated that the tumor growth subtype that reflects the pathologic gross classification was associated with RFS, which is consistent with previous research. A.M. Hui et al demonstrated that the tumor growth subtype of HCC was of clinical value in predicting recurrence and survival after hepatectomy.[13] Likewise, K. Shirabe et al also identified that tumor growth subtype was a prognostic factor for recurrence of HCC in patients undergoing living donor-related liver transplantation (LDLT).[12] Furthermore, a recent study found that tumor growth subtype was related to overall survival (OS) in HCC patients with portal vein tumor thrombus (PVTT).[14] In contrast with single nodular or single nodular with extranodular growth type HCC, confluent multinodular HCC exhibited larger tumor size and poorer differentiation.[15] Our findings further elucidated the prognostic impact of tumor growth subtype in HCC patients without MVI after surgical resection.

The mosaic architecture, an important imaging feature in diagnosing hepatocellular carcinoma, is a significant adverse risk factor for the recurrence of hepatectomy[16] and TACE[17,18] in HCC patients. Consistent with these findings, our study also found that mosaic architecture was significantly associated with poor prognosis in HCC patients without MVI. The mosaic architecture on CT or MRI is featured by randomly appearing nodules or areas within the tumor that vary in enhancement, attenuation, intensity, shape, size, and separation by fibrous tissue.[19] The characteristics behind this appearance may correspond to tumor survival, fatty infiltration, cystic necrosis, hemorrhage, or fibrous tissue in pathological.[20] Thus, mosaic architecture may reflect tumor heterogeneity and rapid disease progression, which may explain why mosaic architecture is responsible for the poor prognosis of HCC patients treated with hepatectomy or TACE.

Internal arteries are often considered an important imaging manifestation of hepatocellular carcinoma, which was identified to be associated with poorly differentiated tumor cells, tumor proliferation, angiogenesis, and stromal invasion.[21] In the previous study, internal arteries are considered an aggressive imaging feature, which has been

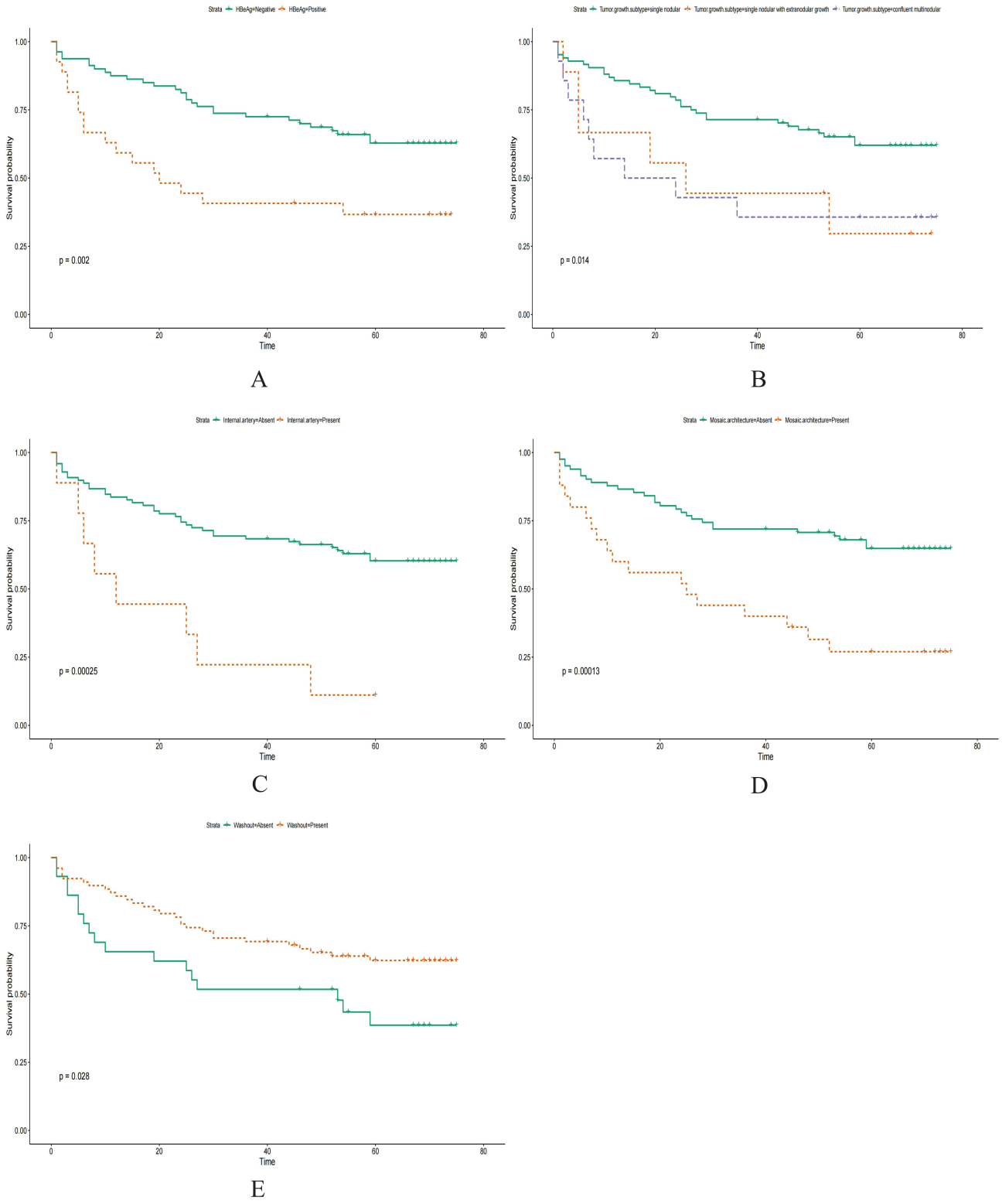

Figure 4 Kaplan–Meier curves of factors for RFS in solitary HCC without MVI. (**A**) HBeAg (positive and negative) (Log rank test, p =0.002). (**B**) Tumor growth subtype (single nodular type, single nodular type with extranodular growth, and multiple confluent nodules) (Log rank test, p =0.014). (**C**) Internal artery (absent and present) (Log rank test, p =0.00025). (**D**) Mosaic architecture (absent and present) (Log rank test, p =0.00013). (**E**) Washout (absent and present) (Log rank test, p =0.028).

confirmed to be a determinant for predicting microvascular invasion[22] and vessels encapsulating tumor clusters (VETC),[23] for diagnosing the macrotrabecular massive (MTM)[24] and high pathological grades[25] in HCC patients. In our study, internal arteries also comprised a risk factor for recurrence in HCC patients without MVI.

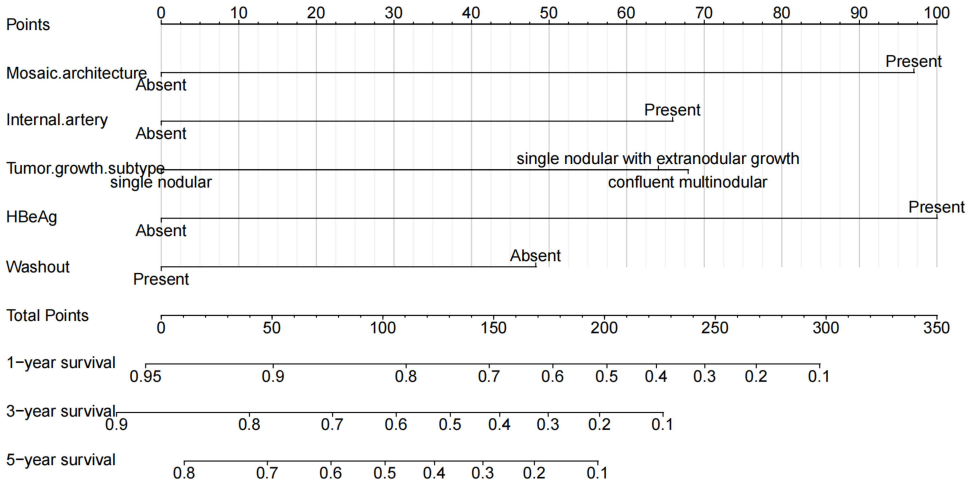

Figure 5 Nomogram of the regression-based model for predicting prognosis for RFS.

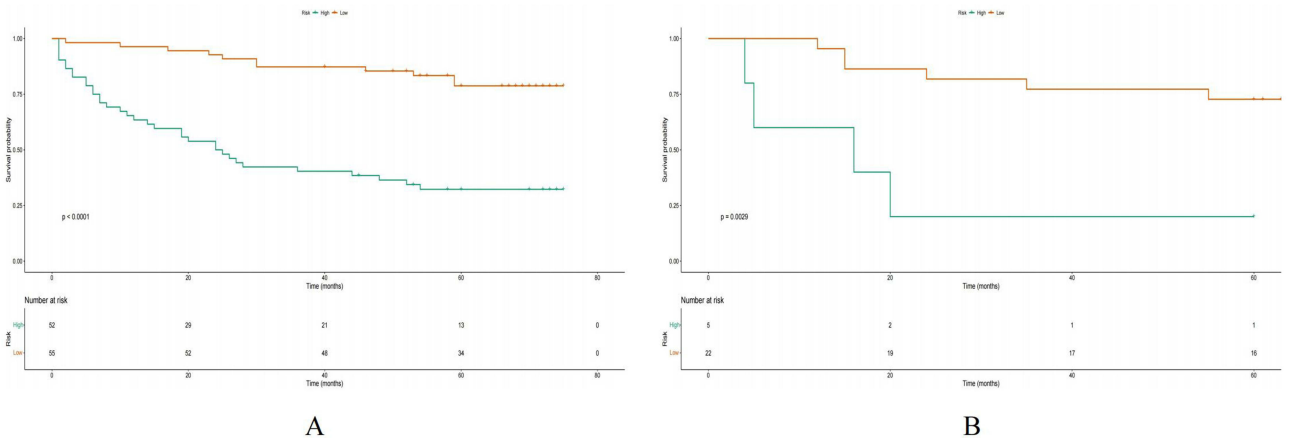

Figure 6 Kaplan–Meier curves of risk stratification postoperative RFS in the training (**A**) and validation (**B**) cohorts.

The liver imaging reporting and data system version 2018 (LI-RADS v2018) classified nonperipheral washout as an LR-5 category; moreover, the prognosis for patients with LR-5 HCC is significantly better than for LR-M.[26] Nonperipheral washout, a significant characteristic in identifying HCC-specific, has previously been associated with relative portal tract reduction pathologically.[27] Zhang et al demonstrated that washout is closely related to better prognosis of HCC patients.[28] Our findings further revealed that nonperipheral washout has a favorable prognosis in HCC patients without MVI. Notably, HBeAg is relevant to the severity of hepatic fibrosis and cirrhosis and is strongly implicated in the recurrence and overall survival of patients with HCC.[29,30] Similarly, HBeAg was also another adverse prognostic marker in our work.

Our study had some limitations. First, this was a retrospective study, which may be subject to sample bias. Second, our finding was validated in the cohort at the branch hospital. Still, there were differences in the follow-up time due to the inconsistent timing of examinations at the two hospital districts. Third, although the prognostic model was carefully considered and internally validated, further multicenter studies are available for external validation. Finally, the follow-up time was not long enough to accurately assess the overall survival of the patients. Therefore, future large-scale multicenter prospective studies evaluating a broader spectrum of HCC patients must be conducted to verify and refine our findings.

Conclusion

In conclusion, we established a straightforward and practical prognostic model utilizing Gd-BOPTA-enhanced MRI to evaluate the postoperative prognosis of single HCC patients without MVI. This model may assist clinicians in stratifying patients into high-risk and low-risk recurrence groups, suggesting intensified clinical surveillance for high-risk patients.

Funding

This work was mainly supported by the key program of Jiangsu Commission of Health (K2023027), the medicine plus X project from Suzhou medical school of Soochow University (grant number ML12203423).

Disclosure

The authors report no conflicts of interest in this work.

References

1. Sung H, Ferlay J, Siegel RL. et al. Global Cancer Statistics 2020: GLOBOCAN Estimates of Incidence and Mortality Worldwide for 36 Cancers in 185 Countries. *CA Cancer J Clin*. 2021;71(3):209–249. doi:10.3322/caac.21660
2. Marrero JA, Kulik LM, Sirlin CB, et al. Diagnosis, staging, and management of hepatocellular carcinoma: 2018 practice guidance by the American Association for the Study of Liver Diseases. *Hepatology*. 2018;68(2):723–750. doi:10.1002/hep.29913
3. Bruix J, Reig M, Sherman M. Evidence-based diagnosis, staging, and treatment of patients with hepatocellular carcinoma. *Gastroenterology*. 2016;150(4):835–853. doi:10.1053/j.gastro.2015.12.041
4. Famularo S, Piardi T, Molfino S, et al. Factors affecting local and intra hepatic distant recurrence after surgery for Hcc: an alternative perspective on microvascular invasion and satellitosis - a Western European Multicentre Study. *J Gastrointest Surg*. 2021;25(1):104–111. doi:10.1007/s11605-019-04503-7
5. Jiang H, Qin Y, Wei H, et al. Prognostic MRI features to predict postresection survivals for very early to intermediate stage hepatocellular carcinoma. *Eur Radiol*. 2024;34(5):3163–3182. doi:10.1007/s00330-023-10279-x
6. Zhang J, Li Y, Xia J, et al. Prediction of Microvascular Invasion and Recurrence After Curative Resection of LI-RADS Category 5 Hepatocellular Carcinoma on Gd-BOPTA Enhanced MRI. *J Hepatocell Carcinoma*. 2024;11:941–952. doi:10.2147/JHC.S459686
7. Tsuboyama T, Onishi H, Kim T, et al. Hepatocellular carcinoma: hepatocyte-selective enhancement at gadoxetic acid-enhanced MR imaging–correlation with expression of sinusoidal and canalicular transporters and bile accumulation. *Radiology*. 2010;255(3):824–833. doi:10.1148/radiol.10091557
8. Tanimoto A, Lee JM, Murakami T, Huppertz A, Kudo M, Grazioli L. Consensus report of the 2nd International Forum for Liver MRI. *Eur Radiol*. 2009;19(S5):S975–S989. doi:10.1007/s00330-009-1624-y
9. Liu C, Sun Y, Yang Y, et al. Gadobenate dimeglumine-enhanced biliary imaging from the hepatobiliary phase can predict progression in patients with liver cirrhosis. *Eur Radiol*. 2021;31(8):5840–5850. doi:10.1007/s00330-021-07702-6
10. Liu C, Shen Z, Ma H, et al. Gd-BOPTA-enhanced hepatobiliary phase MR imaging can predict the prognosis of patients with acute-on-chronic liver failure. *Eur Radiol*. 2022;32(5):3006–3015. doi:10.1007/s00330-021-08440-5
11. Rong D, Liu W, Kuang S, et al. Preoperative prediction of pathologic grade of HCC on gadobenate dimeglumine-enhanced dynamic MRI. *Eur Radiol*. 2021;31(10):7584–7593. doi:10.1007/s00330-021-07891-0
12. Shirabe K, Aishima S, Taketomi A, et al. Prognostic importance of the gross classification of hepatocellular carcinoma in living donor-related liver transplantation. *Br J Surg*. 2011;98(2):261–267. doi:10.1002/bjs.7311
13. Hui AM, Takayama T, Sano K, et al. Predictive value of gross classification of hepatocellular carcinoma on recurrence and survival after hepatectomy. *J Hepatol*. 2000;33(6):975–979. doi:10.1016/S0168-8278(00)80131-2
14. Zhang L, Zheng T, Wu Y, et al. Preoperative MRI-based multiparametric model for survival prediction in hepatocellular carcinoma patients with portal vein tumor thrombus following hepatectomy. *Eur J Radiol*. 2023;165:110895. doi:10.1016/j.ejrad.2023.110895
15. Rhee H, Chung T, Yoo JE, et al. Gross type of hepatocellular carcinoma reflects the tumor hypoxia, fibrosis, and stemness-related marker expression. *Hepatol Int*. 2020;14(2):239–248. doi:10.1007/s12072-020-10012-6
16. Wei H, Fu F, Jiang H, et al. Development and validation of the OSASH score to predict overall survival of hepatocellular carcinoma after surgical resection: a dual-institutional study. *Eur Radiol*. 2023;33(11):7631–7645. doi:10.1007/s00330-023-09725-7
17. Sheng Y, Wang Q, Liu HF, et al. Preoperative nomogram incorporating clinical factors, serological markers and LI-RADS MRI features to predict early recurrence of hepatocellular carcinoma treated with transarterial chemoembolization. *Acad Radiol*. 2023;30(7):1288–1297. doi:10.1016/j.acra.2022.10.020
18. Bao Y, Li JX, Zhou P, et al. Identifying proliferative hepatocellular carcinoma at pretreatment CT: implications for therapeutic outcomes after transarterial chemoembolization. *Radiology*. 2023;308(2):e230457. doi:10.1148/radiol.230457
19. Chen J, Zhou J, Kuang S, et al. Liver imaging reporting and data system category 5: MRI predictors of microvascular invasion and recurrence after hepatectomy for hepatocellular carcinoma. *AJR Am J Roentgenol*. 2019;213(4):821–830. doi:10.2214/AJR.19.21168
20. Cerny M, Chernyak V, Olivié D, et al. LI-RADS Version 2018 Ancillary Features at MRI. *Radiographics*. 2018;38(7):1973–2001. doi:10.1148/rg.2018180052
21. Segal E, Sirlin CB, Ooi C, et al. Decoding global gene expression programs in liver cancer by noninvasive imaging. *Nat Biotechnol*. 2007;25(6):675–680. doi:10.1038/nbt1306
22. Tang Y, Lu X, Liu L, et al. A Reliable and Repeatable Model for Predicting Microvascular Invasion in Patients With Hepatocellular Carcinoma. *Acad Radiol*. 2023;30(8):1521–1527. doi:10.1016/j.acra.2023.02.035

23. Yang J, Dong X, Wang G, et al. Preoperative MRI features for characterization of vessels encapsulating tumor clusters and microvascular invasion in hepatocellular carcinoma. *Abdom Radiol*. 2023;48(2):554–566. doi:10.1007/s00261-022-03740-w
24. Cha H, Choi JY, Park YN, et al. Comparison of imaging findings of macrotrabecular-massive hepatocellular carcinoma using CT and gadoxetic acid-enhanced MRI. *Eur Radiol*. 2022;33(2):1364–1377. doi:10.1007/s00330-022-09105-7
25. Huang K, Dong Z, Cai H, et al. Imaging biomarkers for well and moderate hepatocellular carcinoma: preoperative magnetic resonance image and histopathological correlation. *BMC Cancer*. 2019;19(1):364. doi:10.1186/s12885-019-5574-8
26. Shin J, Lee S, Kim SS, et al. Characteristics and early recurrence of hepatocellular carcinomas categorized as LR-M: comparison with those categorized as LR-4 or 5. *J Magn Reson Imaging*. 2021;54(5):1446–1454. doi:10.1002/jmri.27650
27. Choi JY, Lee JM, Sirlin CB. CT and MR imaging diagnosis and staging of hepatocellular carcinoma: part I. Development, growth, and spread: key pathologic and imaging aspects. *Radiology*. 2014;272(3):635–654. doi:10.1148/radiol.14132361
28. Zhang C, Tao Y, Yang R, Wang Y, Yu Y, Zhou Y. Prediction of Non-Transplantable Recurrence After Liver Resection for Solitary Hepatocellular Carcinoma. *J Hepatocell Carcinoma*. 2024;11:229–240. doi:10.2147/JHC.S412933
29. Hao X, Xu L, Lan X, Li B, Cai H. Impact of hepatic inflammation and fibrosis on the recurrence and long-term survival of hepatitis B virus-related hepatocellular carcinoma patients after hepatectomy. *BMC Cancer*. 2024;24(1):475. doi:10.1186/s12885-024-12187-9
30. Gan L, Ren S, Lang M, et al. Predictive Value of Preoperative Serum AFP, CEA, and CA19-9 Levels in Patients with Single Small Hepatocellular Carcinoma: retrospective Study. *J Hepatocell Carcinoma*. 2022;9:799–810. doi:10.2147/JHC.S376607